AIMETA 2017
XXIII Conference
The Italian Association of Theoretical and Applied Mechanics
Luigi Ascione, Valentino Berardi, Luciano Feo, Fernando Fraternali and Antonio Michele Tralli (eds.)
Salerno, Italy, 4–7 September 2017

VIRTUAL ELEMENT TECHNIQUE FOR COMPUTATIONAL HOMOGENIZATION PROBLEMS

Edoardo Artioli[1], **Sonia Marfia**[2], **Elio Sacco**[2]

[1]Department of Civil Engineering and Computer Science, University of Rome Tor Vergata
Via Politecnico 1, 00133 Roma, Italy
e-mail: artioli@ing.uniroma2.it

[2] Department of Civil and Mechanical Engineering, University of Cassino and Southern Lazio
Via G. Di Biasio 43, 03043 Cassino, Italy
e-mail: {marfia,sacco}@unicas.it

Keywords: Virtual element method, Computational Homogenization, Material Nonlinearity.

Abstract. *In this contribution, the virtual element method (VEM) is adopted for performing homogenization analyses of composites characterized by long fibre inclusions. The homogenization problem is briefly reviewed. Then, the procedure for constructing a virtual element is illustrated. In this context, a new virtual element is proposed for the micromechanical analysis of long fibre composites. It is a plane element, which is able to perform 3D analyses, characterized by three degree of freedom per node that represent the displacement components in the three-dimensional space. Numerical examples are developed for assessing the ability of the VEM in efficiently solving the homogenization problem. Elements characterized by different number of edges are used in the numerical applications.*

1 INTRODUCTION

Composite materials are used in several fields of engineering applications. The development of new and innovative composite materials together with the enhancement of material models and of computational tools promoted the implementation of effective numerical procedures for the accomplishment of sophisticated and accurate stress analyses of composite structural elements.

The issue of the multiscale analysis is very actual in structural mechanics. At the structural level the finite element method is generally adopted. At the material scale a representative volume element (RVE), containing all the peculiarity of the composite material, is studied in order to recover the overall behavior of the composite. To this aim classical analytical homogenization procedures, such as Eshelby, self consistent and Mori Tanaka approach [14], can be adopted. These techniques have also been extended to take into account the nonlinear behavior of the constituents [9, 11]. On the other hand also numerical homogenization techniques can be adopted. In particular, finite element micromechanical analyses could be developed to study the RVE and to determine the overall behavior of the composite. In particular, some micromechanical studies have been proposed in literature to study fibre reinforced composites adopting finite element analyses and taking into account the nonlinear behavior of the composite [8, 12, 13].

Recently, the Virtual Element Method (VEM) has been proposed [1, 6]. It is a new and promising numerical method for solving partial differential equations; it can be viewed as an extension of Finite Element Methods to general polygonal and polyhedral elements. The VEM is characterized by strong mathematical foundations; it is quite simple in implementation and results efficient and accurate in several engineering problems and, in particular, in linear elasticity problems [7, 2]. The VEM has also successfully been applied to solve structural problems characterized by material non-linearity such as plasticity, viscoelasticity and shape memory response [3].

In this paper, the VEM is adopted for performing homogenization analyses of composites characterized by long fibre inclusions. After formulating the homogenization problem, the VEM procedure is illustrated for the specific case of linear polynomial approximation of the displacement fields on the virtual element boundary. A new virtual element is developed for the 3D analyses of long fibre composites. In particular, it is a plane element with three degree of freedoms per node that are the displacement components in the three-dimensional space. Numerical examples are developed for assessing the ability of the VEM in efficiently solving the homogenization problem, validation being provided by comparison with an overkilling finite element solution.

2 HOMOGENIZATION OF LONG FIBRE COMPOSITES

A periodic composite obtained assembling an infinite number of repetitive parallelepiped unit cells (UC) Ω with volume V is considered (cf. Figure 1). The unit cell is characterized by a parallelepiped shape with dimensions equal to $2\,a_1$, $2\,a_2$ and $2\,a_3$ parallel to the three coordinate axes x_1, x_2, x_3. The axis x_3 is parallel to the direction of the fibre axis.

In particular, the repetitive unit cell is obtained considering any possible value of a_3. The 3D

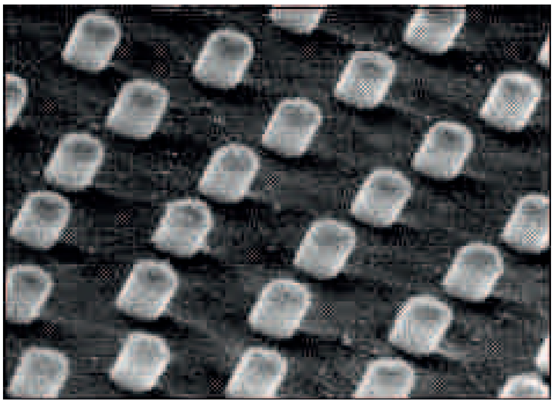

Figure 1: Fibre-reinforced composite material with doubly periodic arrangement of fibres embedded into the matrix.

displacement field for periodic media is expressed by the following representative form:

$$\begin{aligned}
u_1(x_1,x_2,x_3) &= E_{11}\,x_1 + \frac{1}{2}\Gamma_{12}\,x_2 + \frac{1}{2}\Gamma_{13}\,x_3 + u_1^\star(x_1,x_2,x_3) \\
u_2(x_1,x_2,x_3) &= \frac{1}{2}\Gamma_{12}\,x_1 + E_{22}\,x_2 + \frac{1}{2}\Gamma_{23}\,x_3 + u_2^\star(x_1,x_2,x_3) \\
u_3(x_1,x_2,x_3) &= \frac{1}{2}\Gamma_{13}\,x_1 + \frac{1}{2}\Gamma_{23}\,x_2 + E_{33}\,x_3 + u_3^\star(x_1,x_2,x_3)\,,
\end{aligned} \tag{1}$$

where $\mathbf{E} = \{E_{11},\ E_{22},\ E_{33},\ \Gamma_{12},\ \Gamma_{23},\ \Gamma_{13}\}^T$ is the average strain of the UC, $\mathbf{u}^\star = \{u_1^\star,\ u_2^\star,\ u_3^\star\}^T$ is the perturbation displacement, resulting periodic, due to the heterogeneity of the UC while $\mathbf{x} = \{x_1,\ x_2,\ x_3\}^T$ is the position vector of the typical point of Ω. From the formula (1), the strain at the typical point of Ω is:

$$\boldsymbol{\varepsilon}(x_1,x_2,x_3) = \mathbf{E} + \boldsymbol{\varepsilon}^\star(x_1,x_2,x_3)\,, \tag{2}$$

where $\boldsymbol{\varepsilon}^\star$ represents the periodic part of the strain associated with the displacement $\mathbf{u}^\star$ and characterized by null average on the UC. The thickness of the UC in the fibre direction can assume any value thus, imposing the periodicity and continuity conditions along the x_3-direction, it results:

$$\mathbf{u}^\star(x_1,x_2,a_3) = \mathbf{u}^\star(x_1,x_2,-a_3) \qquad \begin{array}{lcl} x_1 & \in & [-a_1,a_1] \\ x_2 & \in & [-a_2,a_2] \end{array} \qquad \forall a_3\,. \tag{3}$$

Thus, from equation (3) the displacement field $\mathbf{u}^\star(x_1,x_2,x_3) = \mathbf{u}^\star(x_1,x_2)$ i.e. it only depends on x_1 and x_2, . The inplane boundary conditions result:

$$\begin{array}{lll} \mathbf{u}^\star(a_1,x_2) & = \mathbf{u}^\star(-a_1,x_2) & x_2 \in [-a_2,a_2] \\ \mathbf{u}^\star(x_1,a_2) & = \mathbf{u}^\star(x_1,-a_2) & x_1 \in [-a_1,a_1] \end{array}\,. \tag{4}$$

The periodic part of the strain is evaluated as $\boldsymbol{\varepsilon}^\star = \boldsymbol{\varepsilon}\left(\mathbf{u}^\star\right)$, resulting:

$$\boldsymbol{\varepsilon}^\star = \mathbf{L}\mathbf{u}^\star = \left\{ \begin{array}{c} u_{1,1}^\star \\ u_{2,2}^\star \\ 0 \\ u_{1,2}^\star + u_{2,1}^\star \\ u_{3,2}^\star \\ u_{3,1}^\star \end{array} \right\} \quad \text{with} \quad \mathbf{L} = \left[\begin{array}{lll} \cdot_{,1} & 0 & 0 \\ 0 & \cdot_{,2} & 0 \\ 0 & 0 & 0 \\ \cdot_{,2} & \cdot_{,1} & 0 \\ 0 & 0 & \cdot_{,2} \\ 0 & 0 & \cdot_{,1} \end{array} \right]\,, \tag{5}$$

as all the derivatives with respect to x_3 are zero, because the displacement components do not depend on x_3.

The local stress field is defined as:

$$\boldsymbol{\sigma}(x_1, x_2) \quad = \mathbf{C}(x_1, x_2)\boldsymbol{\varepsilon}(x_1, x_2)\,, \tag{6}$$

where $\mathbf{C}$ is the elastic matrix that assumes a different value in the fibre and in the matrix.

The average stress in the UC is evaluated as:

$$\boldsymbol{\Sigma} = \frac{1}{V}\int_{\Omega} \boldsymbol{\sigma}\, dV\,. \tag{7}$$

3 VIRTUAL ELEMENT METHOD

The virtual element VE formulation is briefly presented in this section. First, a polygonal discretization of the unit cell Ω is performed, considering non overlapping polygons Ω_E characterized by a number m of straight edges e. The space of the approximated displacement field is defined element-wise by introducing local degrees of freedom, as in standard FE method, but differently from FE, the definition of the local displacement approximation is not fully explicit [7, 2]. Different accuracy can be introduced in the method, depending on the degree k of the approximating functions for the displacement field. Next, the $i-$th component of the approximated displacement field is denoted as u_i^h.

To construct a virtual element for the problem described in the previous section, the procedure schematically described below can be performed.

1. The number m of edges defining the VE is set.

2. The displacements are approximated assuming an explicit representation of their components only on the boundary of each virtual element Ω_E. Let the displacement approximation be denoted by $\mathbf{u}^{\star h}$, with h related to the mesh size, whose corresponding displacement on the boundary $\partial\Omega_E$ of the VE is $\tilde{\mathbf{u}}^{\star h}$; it is assumed that the typical component of the displacement on the VE boundary is approximated by a polynomial of degree k, i.e. $\tilde{u}_i^{\star h} \in P_k(e)$, so that it can be written:

$$\tilde{\mathbf{u}}^{\star h} = \mathbf{N}\,\mathbf{U}^{\star}\,, \tag{8}$$

   with $\mathbf{N}$ a matrix containing the approximation functions and $\mathbf{U}^{\star}$ the vector collecting the nodal degree of freedom.
   In particular, herein it is set $k = 1$, so that $\tilde{u}_i^{\star h} \in P_1(e)$ i.e. the displacement components are linear functions along the polygonal edges.

3. The equilibrium equation, written in the approximated variational form for the single VE, is expressed as:

$$0 = \int_{\Omega_E} [\boldsymbol{\varepsilon}(\delta\mathbf{u}^{\star h})]^T\, \mathbf{C}\, [\boldsymbol{\varepsilon}(\mathbf{u}^{\star h}) + \mathbf{E}]\, dA\,. \tag{9}$$

4. As the approximated displacement field $u_i^{\star h}$ is not defined inside the element, but only on the boundary $\partial\Omega_E$, the gradient cannot be computed and, consequently, an explicit

expression of strain is not available. Thus, a projector operator Π is introduced to evaluate the strain associated to the displacement field. It is defined on the basis of the two fundamental requirements:

$$\begin{aligned} \Pi(u_i^{\star h}) \quad & \in P_{k-1}(\Omega_E) = P_0(\Omega_E) \\ 0 \quad & = \int_{\Omega_E} (\boldsymbol{\varepsilon}^P)^T \left[\Pi(\mathbf{u}^{\star h}) - \boldsymbol{\varepsilon}(\mathbf{u}^{\star h}) \right] dA \qquad \forall \boldsymbol{\varepsilon}^P \in P_0(\Omega_E) \,, \end{aligned} \tag{10}$$

so that the strain components are approximated by a constant function in each VE.

5. Integrating by parts, equation $(10)_2$ becomes:

$$\begin{aligned} & \int_{\Omega_E} (\boldsymbol{\varepsilon}^P)^T \, \Pi(\mathbf{u}^{\star h}) \, dA = \int_{\Omega_E} (\boldsymbol{\varepsilon}^P)^T \, \boldsymbol{\varepsilon}(\mathbf{u}^{\star h}) \, dA = \\ & \int_{\Omega_E} (\boldsymbol{\varepsilon}^P)^T \, \mathbf{L} \, \mathbf{u}^{\star h} \, dA = \int_{\partial\Omega_E} (\boldsymbol{\varepsilon}^P)^T \, \mathbf{N}_E \, \tilde{\mathbf{u}}^{\star h} \, dA - \int_{\Omega_E} (\mathbf{L}^T \, \boldsymbol{\varepsilon}^P)^T \, \mathbf{u}^{\star h} \, dA = \\ & \int_{\partial\Omega_E} (\boldsymbol{\varepsilon}^P)^T \, \mathbf{N}_E \, \tilde{\mathbf{u}}^{\star h} \, dA \qquad \qquad \forall \boldsymbol{\varepsilon}^P \in P_0(\Omega_E) \,, \end{aligned} \tag{11}$$

where the term $\mathbf{L} \, \boldsymbol{\varepsilon}^P = \mathbf{0}$ as $\boldsymbol{\varepsilon}^P \in P_0(\Omega_E)$ and $\mathbf{N}_E$ is the matrix containing the components of the outward normal to the element boundary:

$$\mathbf{N}_E = \begin{bmatrix} n_1 & 0 & 0 \\ 0 & n_2 & 0 \\ 0 & 0 & 0 \\ n_2 & n_1 & 0 \\ 0 & 0 & n_2 \\ 0 & 0 & n_1 \end{bmatrix} . \tag{12}$$

6. As the integral in the last right hand side of equation (11) is performed only on the boundary of the element, the approximation (8) can be accounted for, obtaining:

$$\int_{\Omega_E} (\boldsymbol{\varepsilon}^P)^T \, \Pi(\mathbf{u}^{\star h}) \, dA = \int_{\partial\Omega_E} (\boldsymbol{\varepsilon}^P)^T \, \mathbf{N}_E \, \mathbf{N} \, dA \; \mathbf{U}^\star \qquad \forall \boldsymbol{\varepsilon}^P \in P_0(\Omega_E) \,. \tag{13}$$

7. Accounting that for $k = 1$ the strain $\boldsymbol{\varepsilon}^P$ results constant in Ω_E, and setting $\Pi(\mathbf{u}^{\star h}) = \boldsymbol{\Pi}^m \, \mathbf{U}^\star$, equation (13) leads to:

$$(\boldsymbol{\varepsilon}^P)^T \, \boldsymbol{\Pi}^m \, \mathbf{U}^\star A_E = (\boldsymbol{\varepsilon}^P)^T \int_{\partial\Omega_E} \mathbf{N}_E \, \mathbf{N} \, dA \; \mathbf{U}^\star \qquad \forall \boldsymbol{\varepsilon}^P \in P_0(\Omega_E) \tag{14}$$

that gives:

$$\boldsymbol{\Pi}^m = \frac{1}{A_E} \int_{\partial\Omega_E} \mathbf{N}_E \, \mathbf{N} \, dA \,, \tag{15}$$

where A_E is the area of Ω_E.

8. Once the projection operator $\boldsymbol{\Pi}^m$ is evaluated, the equilibrium equation (9) takes the form:

$$\mathbf{0} = (\mathbf{K}_c + \mathbf{K}_S) \, \mathbf{U}^\star + \mathbf{B} \,, \tag{16}$$

where

$$\mathbf{K}_c = (\mathbf{\Pi}^m)^T \, \mathbf{C} \, \mathbf{\Pi}^m \, A_E \qquad (17)$$
$$\mathbf{B} = (\mathbf{\Pi}^m)^T \, \mathbf{E} \, A_E \qquad (18)$$

and $\mathbf{K}_S$ is a stiffness matrix coming from a suitable stabilization term, needed to preserve the coercivity of the system.

9. To determine the stabilization term, it is assumed that each component of the approximated form of the displacement field can be represented as linear function of the in-plane coordinates (x_1, x_2), so that $u_i^{\star h} \in (P_1(E))^3$ with:

$$(P_1(E))^3 = \left\{ \begin{array}{ccccccccc} 1 & 0 & 0 & x_1 & 0 & 0 & x_2 & 0 & 0 \\ 0 & 1 & 0 & 0 & x_1 & 0 & 0 & x_2 & 0 \\ 0 & 0 & 1 & 0 & 0 & x_1 & 0 & 0 & x_2 \end{array} \right\} . \qquad (19)$$

4 NUMERICAL APPLICATIONS

The present section is devoted to validation and accuracy assessment of the proposed VEM technology. As it is commonly accepted the majority of modern advanced composite materials with fibre reinforcement are based on components characterized by complex material constitutive behavior and possibly general fibre arrangements into the unit cell [5, 4]. In this regard, an efficient, reliable numerical tool for computing overall properties of such composites is of great importance from technical point of view, since analytical or semi-analytical methods are practically not available for the more complex material setups [10], as for instance randomly distributed fibres.

With reference to a family of composites characterized by square unit cells and different volume fractions, the previously introduced method is applied to compute the effective material moduli. Material parameters for the fibre and for the matrix are $E^f = 4.1 \; 10^5 \mathrm{N/mm}^2$, $\nu^f = 0.19$, $E^m = 0.75 \; 10^5 \mathrm{N/mm}^2$, $\nu^m = 0.33$, respectively. Volume fractions values taken into consideration are $v_f = 0.2, \; 0.4, \; 0.6$. The numerical campaign is conducted comparing the results obtained adopting three types of VEM simple meshes over the unit cell domain; in particular, triangles, polygons, and quadrilaterals, as illustrated in Fig. 2 are considered. A reference solution is here computed with an overkilling mesh of triangular linear finite elements, which noticeably coincide with the linear triangular VEM counterpart, i.e. $m = 3$, $k = 1$.

	Tri	Poly	Quad
Mesh 1	293	144	201
Mesh 2	925	576	689
Mesh 3	3417	2304	2529
Mesh 4	13109	9216	9665
Overkilling	149249	-	-

Table 1: Meshing discretizations in terms of number of vertices for examined case $v_f = 0.4$.

Error measures are reported in the following in terms of:

- $\mathcal{E}_{ij}$: relative error on the $ij-th$ average stress component $\bar{\Sigma}_{ij}$ due to the average strain component E_{ij}

- $\mathcal{E}_{\bar{C}}$: Euclidean error norm on effective moduli $\bar{C}$
- $\mathcal{E}_{\bar{\Sigma}_{Mises}}$: Euclidean error norm on Mises average stress $\bar{\Sigma}_{Mises}$ associated to $\bar{\Sigma}$ due to the average strain component E_{11}

Figure 3 reports the above error measures for the three compared methods, adopting an overkilling solution obtained with VEM triangles of order 1, in the intermediate case $v_f = 0.40$, while details on mesh discretization are given in Table 1. Noticeably, the three methods compare favorably with similar error levels while amongst the tested element types triangles seems to perform best on the overall. This confirm the interesting reliability properties of the proposed methodology in particular when triangular meshing is required, i.e. when complex geometries are investigated, as it is the case of a unit cell close to the packaging limit, for instance. Figures 4-5 report the same error level comparison for the other two unit cell configurations, i.e. $v_f = 0.20$, and $v_f = 0.60$, confirming the reliability of the proposed methodology which may serve as a powerful versatile technique to compute the overall material response of the composite.

Figure 6 reports error measures $\mathcal{E}_{ij}$ on relevant $ij = 11,\ 33,\ 44,\ 66$ effective stress components when the elastic shear moduli contrast factor $\eta = G^f/G^m$ varies from 10^{-3} to 10^3. The reference overkilling solution is still computed with first order VEM triangles. The computed solutions seem relatively insensitive to the above material heterogeneity parameter ξ, confirming the robustness of the proposed VEM methodology.

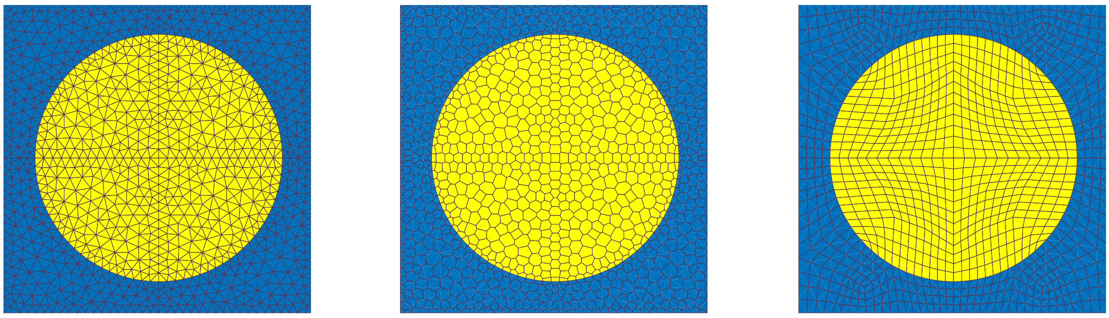

(a) (b) (c)

Figure 2: Sample unit cell meshes for examined case $v_f = 0.4$. (a) triangles; (b) polygons; (c) quadrilaterals.

5 CONCLUSIONS

- A virtual element method of order $k = 1$ has been presented for the homogenization of fibre-reinforced composite materials with doubly periodic square lattices and circular fibre inclusions;
- The methodology has been tested and validated on a number of unit cell setups for triangular, quadrilateral and Voronoi tessellations mesh types;
- The strength of the proposed approach relies in the ability to accurately deal with complex geometries, flexibility in mesh generation and local adaptive refinement, and polynomial degree elevation;
- Future investigations of this study include treatment of complex material constitutive behavior, general representative unit cells and the case of complex inclusion shapes.

- Preliminary results on the extension to $k = 2$ VEM approximation spaces for the problem treated in the present work indicate a superior behavior, in terms of accuracy and efficiency, with respect to quadratic standard Lagrangian isoparametric 2D finite elements. Such results will be the object of further communication.

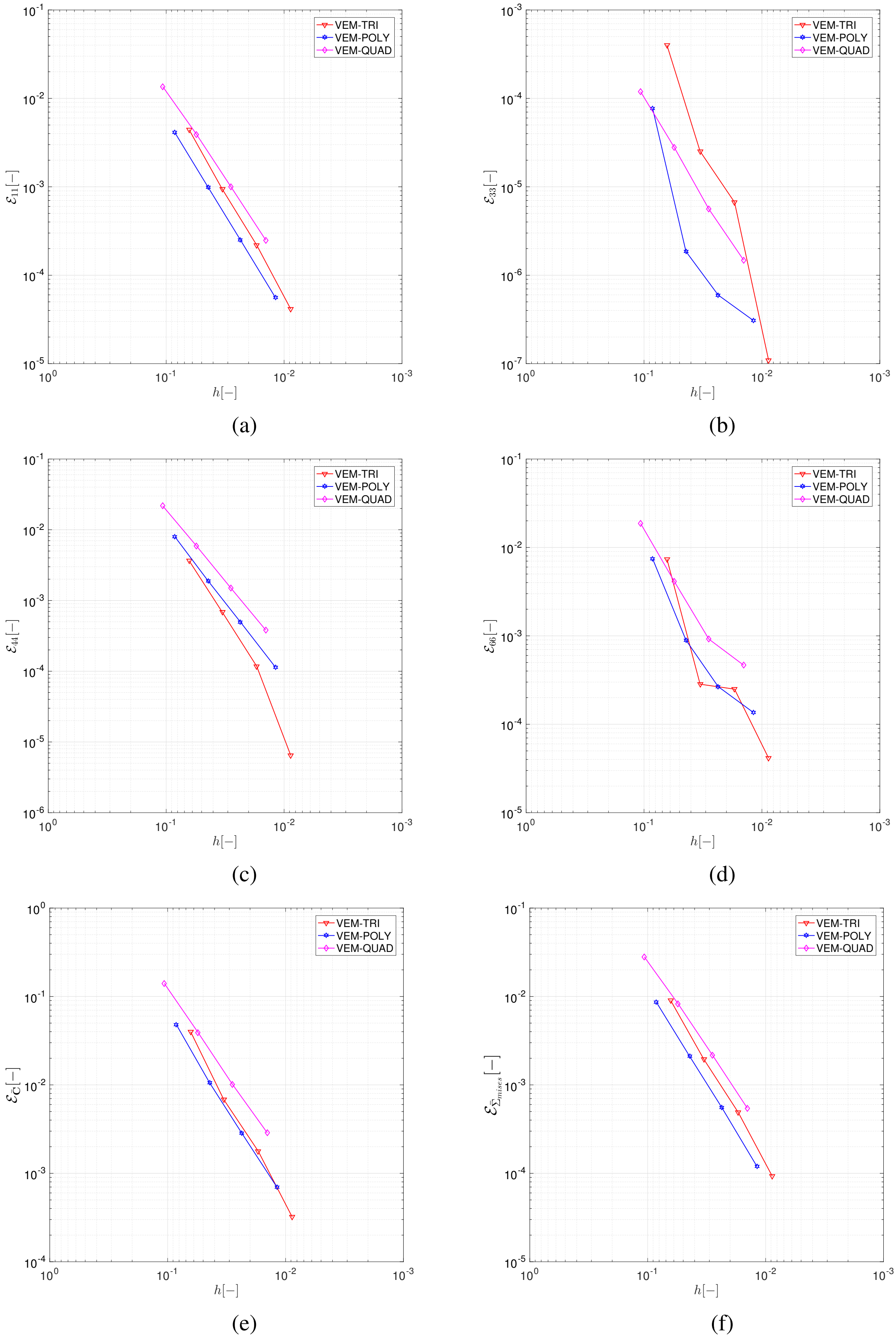

Figure 3: Accuracy assessment for various error measures. Square unit cell, $v_f = 0.40$. Compared methods: VEM with triangles, polygons, quadrilaterals; reference overkilling solution computed with FEM linear triangles.

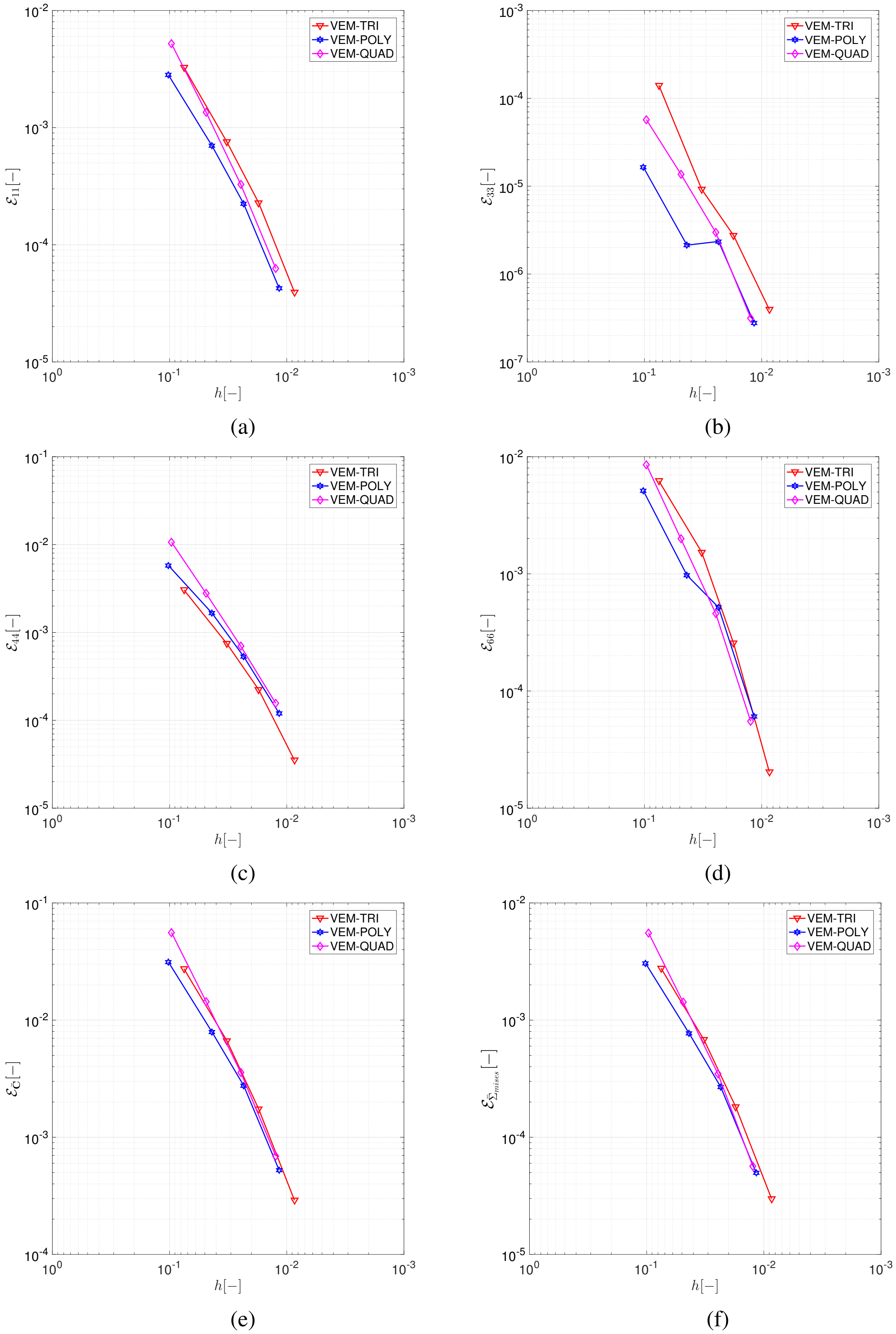

Figure 4: Accuracy assessment for various error measures. Square unit cell, $v_f = 0.20$. Compared methods: VEM with triangles, polygons, quadrilaterals.

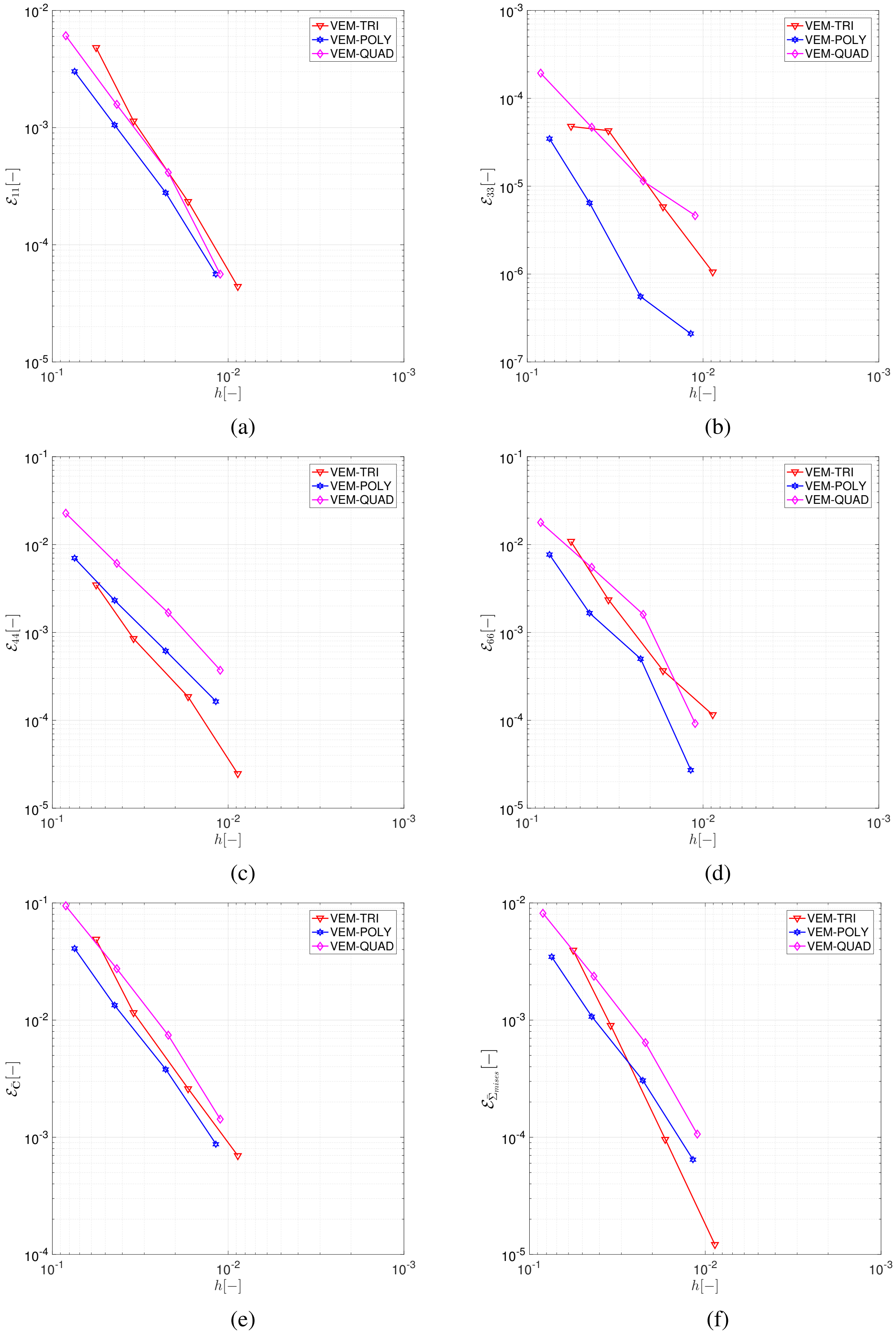

Figure 5: Accuracy assessment for various error measures. Square unit cell, $v_f = 0.60$. Compared methods: VEM with triangles, polygons, quadrilaterals.

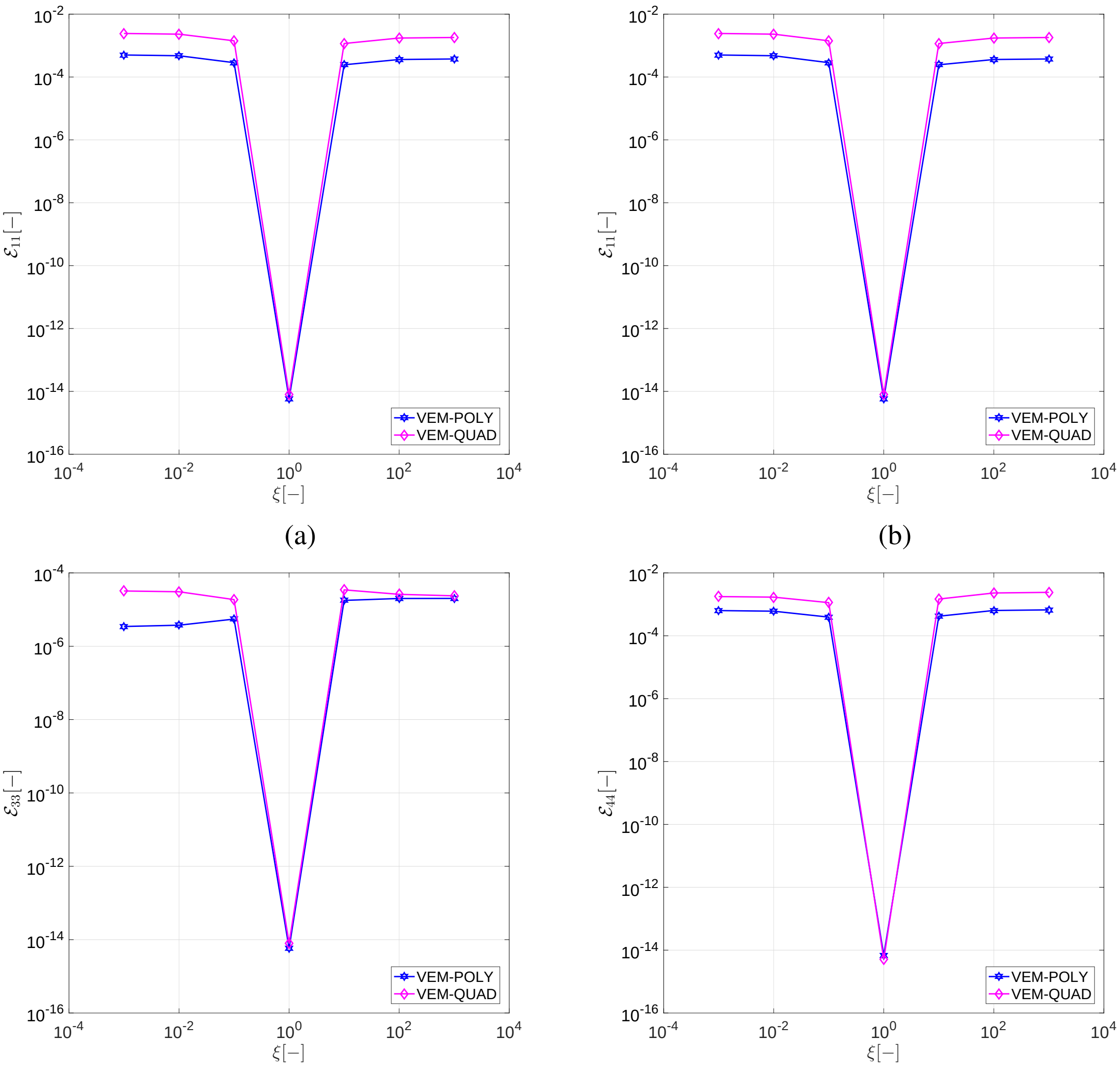

Figure 6: Sensitivity of the solution with respect to the contrast parameter η. Square unit cell, $v_f = 0.40$. Compared methods: VEM with polygons, quadrilaterals.

REFERENCES

[1] B. Ahmad, A. Alsaedi, F. Brezzi, L. D. Marini, and A. Russo, *Equivalent projectors for virtual element methods*, Comput. Math. Appl. **66** (2013), no. 3, 376–391.

[2] E. Artioli, L. Beirão da Veiga, C. Lovadina, and E. Sacco, *Arbitrary order 2D virtual elements for polygonal meshes: Part I, elastic problem*, Computational Mechanics (2017), doi:10.1007/s00466–017–1404–5.

[3] E. Artioli, L. Beirão da Veiga, C. Lovadina, and E. Sacco, *Arbitrary order 2D virtual elements for polygonal meshes: Part II, inelastic problem*, Computational Mechanics (2017), doi:10.1007/s00466–017–1429–9.

[4] E. Artioli and P. Bisegna, *Effective longitudinal shear moduli of periodic fibre-reinforced composites with functionally-graded fibre coatingss*, Int. J. Solids Struct. **50** (2013), 1154–1163.

[5] E. Artioli, P. Bisegna, and F. Maceri, *Effective longitudinal shear moduli of periodic fibre-reinforced composites with radially-graded fibres*, Int. J. Solids Struct. **47** (2010), 383–397.

[6] L. Beirão da Veiga, F. Brezzi, A. Cangiani, G. Manzini, L. D. Marini, and A. Russo, *Basic principles of virtual element methods*, Math. Models Methods Appl. Sci. **23** (2013), no. 1, 199–214.

[7] L. Beirão da Veiga, F. Brezzi, and L. D. Marini, *Virtual elements for linear elasticity problems*, SIAM J. Numer. Anal. **51** (2013), no. 2, 794–812.

[8] V. Carvelli and A. Taliercio, *Micromechanical model for the analysis of unidirectional elasto-plastic composites subjected to 3D stresses.*, Mechanical Research Communications **26** (1999), 547 – 553.

[9] C. Czarnota, K. Kowalczyk-Gajewska, A. Salahouelhadj, M. Martiny, and S. Mercier, *Modeling of the cyclic behavior of elastic-viscoplastic composites by the additive tangent Mori-Tanaka approach and validation by finite element calculations*, International Journal of Solids and Structures **56-57** (2015), 96 – 117.

[10] D. Joyce, W.J. Parnell, R.C. Assier, and I.D. Abrahams, *An integral equation method for the homogenization of unidirectional fibre-reinforced media; antiplane elasticity and other potential problems*, accepted, and online on: http://rspa.royalsocietypublishing.org/ (2017).

[11] C. Mareau and S. Berbenni, *An affine formulation for the self-consistent modeling of elasto-viscoplastic heterogeneous materials based on the translated field method*, International Journal of Plasticity **64** (2015), 134 – 150.

[12] S. Marfia, *Micro-macro analysis of shape memory alloy composites*, Int. J. of Solids Struct. **42** (2005), 3677–3699.

[13] S. Marfia and E. Sacco, *Micromechanics and homogenization of sma-wire-reinforced materials*, Journal of Applied Mechanics **72** (2005), 259–268.

[14] T. Mura, *Micromechanics of defects in solid*, Martinus, 1987.